


Acoustic resonators: Symmetry classification and multipolar content of the eigenmodes

Mariia Tsimokha, Vladimir Igoshin , Anastasia Nikitina , Ivan Toftul ^{*}, Kristina Frizyuk [†], and Mihail Petrov
The School of Physics and Engineering, ITMO University, St. Petersburg 197101, Russia



(Received 23 October 2021; revised 14 March 2022; accepted 6 April 2022; published 28 April 2022)

Acoustics recently became a versatile platform for discovering novel physical effects and concepts at a relatively simple technological level. In this way, single resonators and the structure of their resonant modes play a central role and define the properties of complex acoustic systems such as acoustic metamaterials, phononic crystals, and topological structures. In this paper, we present a powerful method allowing a qualitative analysis of eigenmodes of resonators in the linear monochromatic acoustic domain based on multipole classification of eigenmodes. Using the apparatus of group theory, we explain and predict the structure of the scattered field knowing only the symmetry group of the resonator by connecting the multipolar content of incident and scattered fields. Such an approach can be utilized for developing resonators with predesigned properties avoiding time-consuming simulations. We performed full multipole symmetry classification for a number of resonator geometries and tightened it with scattering spectra profiles.

DOI: [10.1103/PhysRevB.105.165311](https://doi.org/10.1103/PhysRevB.105.165311)

I. INTRODUCTION

Studying acoustic resonators is essential both for many technological applications and for fundamental research developing acoustic metamaterials with established properties [1–9], various optomechanical systems [10,11], topological insulators [12,13], and achieving bound states in the continuum [14,15]. One of the most important characteristics of any resonator is its eigenmode spectrum and their field structure. Commonly, they are examined with full-wave numerical simulations, while analytical solutions can be obtained solely for a limited number of resonator shapes. A spherical scatterer is one of the examples and the plane-wave scattering on an arbitrary size sphere [16,17] was considered for the first time more than 150 years ago by Clebsch [18] and Lorentz [19] for elastic waves, which in electro-magnetic theory is well known as Mie scattering [20]. However, the unified description of eigenmodes in an acoustic resonator of arbitrary shape has not been made so far. In solid-state physics, quantum chemistry, optics, and elastodynamics a powerful method based on group theory analysis has been widely utilized [21–28]. The mode structure is defined solely by the symmetry of the system and can be classified by the irreducible representations (irreps) of the system's symmetry group. The symmetry of the eigenmodes can also give an answer on which modes are involved in physical processes such as linear and nonlinear wave scattering, also referred to as selection rules [29–35]. We build our approach on multipole decomposition of acoustic waves. Generally, the multipole expansion is actively used in nanophotonics [36–39] and demonstrated that it can be effectively used for predicting the optical properties of sub-wavelength resonators. In acoustics the multipole approach

was also well known for decades, but drew much attention recently gaining a second wave of popularity [40–50], enabling effective control over the wave-propagation directions and radiation reaction forces [11,51–56].

In our paper, we provide classification and multipole expansion of an acoustic resonators' eigenmodes of various symmetry, as well as its application to the acoustic scattering (see Fig. 1). We hope that this work will bring a beneficial addition to the growing body of literature that employs group theory to analyze the elastodynamics of complex systems of various levels of geometrical symmetry [28,57–59]. Throughout this work we will discuss only longitudinal acoustic pressure waves in a monochromatic domain [60]. Inspired by the recent progress in nanophotonics, we will operate in terms of a spherical harmonics (multipoles) basis analyzing their symmetry [61–64], which could be even simpler and more efficient due to the scalar origin of fields. We show how to connect the symmetry of the resonator with the particular multipolar components of each eigenmode. Based on this, one can immediately interpret and predict the scattering spectra, directivity of the scattering, and even acoustics forces acting on resonators due to the interaction with an arbitrary incident wave.

The paper is constructed as follows. In Sec. I we give an introductory part, which designates the paper's place in the current state of linear acoustics and optics. In Sec. II we give some helpful basis of group theory, which is necessary for the understanding of the main results. In Sec. III we apply our analysis to a particular case of D_{3h} symmetry group resonators, which can be similarly applied to other symmetries. Then we discuss, what happens with the eigenmodes when lowering the symmetry. In Sec. IV we discuss an influence of the resonators' symmetry on the cross section of the scattered wave. Finally, in Sec. V we compare it with the case of optical resonators, while demonstrating some similarities and dissimilarities, eventually revealing ways of better understanding both types of scattering and other processes.

^{*}toftul.ivan@gmail.com

[†]k.frizyuk@metalab.ifmo.ru

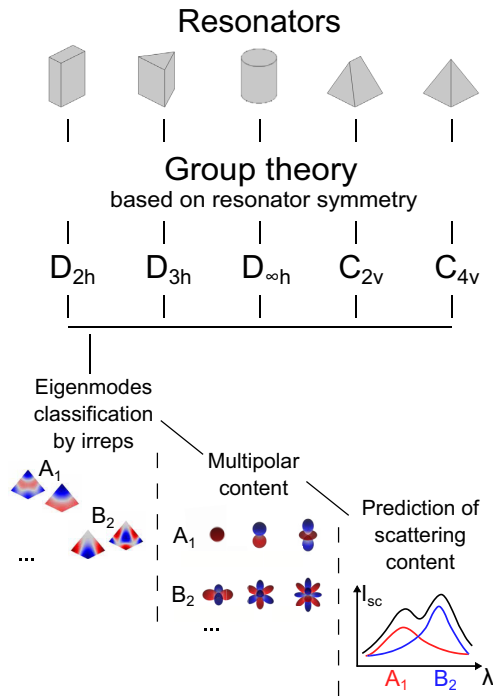


FIG. 1. The general approach and step-by-step algorithm to analysis of acoustic resonators modes suggested in this work.

II. BASICS OF GROUP SYMMETRY AND ACOUSTIC MODES ANALYSIS

In our work, we discuss a system with a particular symmetry, i.e., an acoustic resonator or scatterer with a symmetric shape. We will show how symmetry provides information about eigenmodes and their multipolar content. For better understanding of the theory a brief summary of several topics is presented below. Here we will introduce the concepts of irreducible representation, functions transformed under irreducible representation (basis of the representation), spherical harmonics, multipole expansion, and Wigner theorem.

A. Group and representation theory

Group is a set equipped with a binary operation that holds three axioms: associativity, identity, and invertibility. The following study focuses mainly on the systems' symmetry groups that consist of the elements that transform the system to itself, i.e., symmetry operations [66]. Group elements are symmetry operations: rotations and reflections of the resonator. A representation of a group \mathbf{G} on a vector space \mathbb{V} is a homomorphism T of \mathbf{G} to the group of automorphisms of \mathbb{V} : $GL(\mathbb{V})$ [67]

$$T: \mathbf{G} \rightarrow GL(\mathbb{V}).$$

In simpler words, group representation is a matrix group with square matrices, where we assign a matrix $D(g)$ to each element $g \in G$ such that $D(g_1 g_2) = D(g_1) D(g_2)$, i.e., the matrices satisfy the group's multiplication table [23]. Representation is considered irreducible if there is no nontrivial invariant subspace in space \mathbb{V} [22,23]. In other words, all matrices $D(g)$ of any representation can be simultaneously

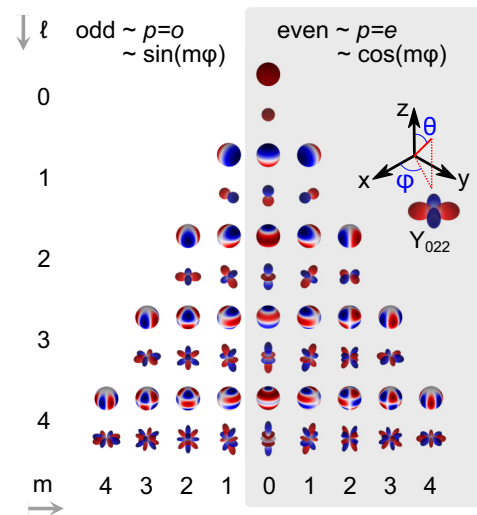


FIG. 2. The real spherical functions $Y_{p\ell m}(\theta, \varphi)$ up to $\ell = 4$. At the top of the line the color shows the value of the function depending on the angles θ, φ , the graph is shown on the sphere. At the bottom the radius of the sphere is deformed in proportion to the modulus of the function value.

reduced (by a linear basis transformation) to a block-diagonal form, which consists of irreducible blocks that turn out to be, in fact, irreducible representations of that group [23].

The term *set of functions* $\psi_i(\mathbf{r})$ transforming through each other under the irreducible representation (or the basis of representation) describes that after the group element action (rotations or reflections in our case) functions are transformed to the particular linear combinations of themselves (from the same set)

$$\psi_i(g^{-1}\mathbf{r}) = \sum_j D_{ji}(g)\psi_j(\mathbf{r}). \quad (1)$$

To illustrate it, let us introduce spherical harmonic functions also referred to as multipoles. A real form in terms of complex spherical harmonics (Fig. 2) is set as [53,68]

$$Y_{p\ell m} = \begin{cases} \frac{i}{\sqrt{2}}[Y_\ell^{-m} - (-1)^m Y_\ell^m] & p = o, \\ Y_\ell^0 & m = 0, \\ \frac{1}{\sqrt{2}}[Y_\ell^{-m} + (-1)^m Y_\ell^m] & p = e. \end{cases} \quad (2)$$

Spherical functions with a particular ℓ are basis functions of $2\ell + 1$ -dimensional irreducible representation of the rotation group of sphere $SO(3)$, therefore under an arbitrary angle rotation they transform into the linear combination of functions with the same ℓ (Fig. 3) [65].

The results of our work are based on a Wigner's theorem [69]. It is formulated as follows:

$$\mathcal{H}(\mathbf{r})\psi(\mathbf{r}) = \epsilon\psi(\mathbf{r}). \quad (3)$$

Suppose that an eigenvalue equation, describing a system, is invariant under the transformations of a symmetry group, then the eigenfunctions are transformed under irreducible representations of the group.

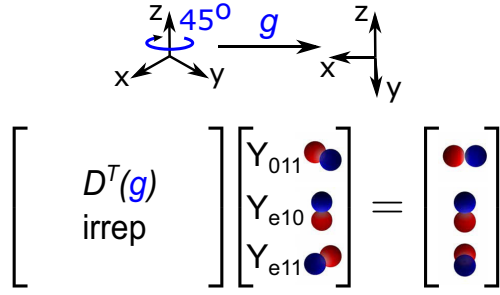


FIG. 3. Spherical functions with $\ell = 1$ transforming through each other under the three-dimensional irreducible representation. For complex form of spherical harmonics $D(g)$ matrix can be obtained using Wigner D -matrixes [65].

In other words, each eigenvalue ϵ corresponds to a particular irrep, and functions $\psi(\mathbf{r})$, which transform through each other under a particular irrep, correspond to the same eigenvalue.

Let us apply this formalism to the linear acoustics in the monochromatic domain with frequency ω . The main variables are *pressure* $p = p(\mathbf{r}, \omega)$ and *velocity* $\mathbf{v} = \mathbf{v}(\mathbf{r}, \omega)$ fields which satisfy $i\omega\beta p = \nabla \cdot \mathbf{v}$ (the equation of continuity or mass conservation law) and $i\omega\rho\mathbf{v} = \nabla p$ (the linearized Navier-Stokes equation) [70–72]. Throughout this paper we use complex amplitudes p, \mathbf{v} which are connected with the real observable fields $\mathfrak{p}, \mathfrak{v}$ as $[\mathfrak{p}, \mathfrak{v}](\mathbf{r}, \mathbf{t}) = \text{Re}([p, \mathbf{v}](\mathbf{r}, \omega)e^{-i\omega t})$. The medium is characterized by compressibility $\beta = \beta(\mathbf{r})$ and density $\rho = \rho(\mathbf{r})$. As a consequence of the master equations, the pressure field satisfies the equation

$$-c^2(\mathbf{r})\nabla^2 p = \omega^2 p, \quad c(\mathbf{r})^2 = \frac{1}{\beta(\mathbf{r})\rho(\mathbf{r})}, \quad (4)$$

here $c(\mathbf{r})$ is the coordinate-dependent speed of sound and the operator $\mathcal{H}(\mathbf{r}) \equiv -c^2(\mathbf{r})\nabla^2$. For part of space in which $c(\mathbf{r}) = \text{const.}(\mathbf{r})$ Eq. (4) reduces to the well-known Helmholtz equation. Here we neglected an extra term, which takes place due to the $\nabla\rho \neq 0$ (see Appendix A). This can be done once the boundary conditions are carefully considered.

From the Wigner's theorem it immediately follows that the degree of degeneracy of an eigenmode equals the dimension of the corresponding irreducible representation. One of the simplest examples of this approach is that the angular dependence of the each spherical resonator's mode can be portrayed as a particular spherical function (Fig. 2) [23], while modes with identical ℓ are $(2\ell + 1)$ -degenerate.

B. Multipole expansion of resonators' eigenmodes

While the eigenmodes of a spherical resonator are defined by only one spherical harmonic, the situation becomes much more complex for the resonators of an arbitrary shape. Now their modes cannot be defined by a specific spherical harmonic, but rather can be decomposed over a multipoles' set. At this stage, defining the multipole content becomes a complex numerical problem, however, one immediately identifies it using *Wigner's theorem*. Indeed, the modes' behavior under all symmetry transformations defines under which irreducible

representation it transforms. Now the multipoles contained in the mode should only belong to the same irreducible representation. Thus, one needs to know under which irrep of the resonator's symmetry group each spherical harmonics transforms.

III. THEORY AND RESULTS OF MULTIPOLE EXPANSION

A. Multipole analysis using group theory

If there is an acoustic resonator with a defined symmetry, then the equation describing the system is invariant under the symmetry transformations of the group. Any finite resonator can be considered as a perturbation of a spherical resonator [73,74]. Its eigenmodes can be compounded of the sphere's eigenmodes.

In this section, we restrict ourselves to assessing the hard boundary condition $\partial_n p|_{\partial\Omega} = 0$ at the resonator surface. Alternatively, the radiative, Sommerfeld-type boundary condition at $r \rightarrow \infty$ can also be assessed. Such open resonators appear when one ponders scattering problems. However, from the symmetry point of view they will provide the same result: the symmetry of the eigenmodes and their multipolar content will be the same.

Let us consider a particular eigenmode of an acoustic resonator which is described by a complex amplitude of pressure $p(\mathbf{r}, \omega)$. We can write a multipole decomposition as a sum of scalar spherical functions [75]

$$p(\mathbf{r}, \omega) = \sum_{p,\ell,m} b_{p\ell m}(r, \omega) Y_{p\ell m}(\theta, \varphi), \quad (5)$$

where the summation is taken over all the indexes as follows: $\sum_{p,\ell,m} \equiv \sum_{p=e,o} \sum_{\ell=0}^{\infty} \sum_{m=-\ell}^{\ell}$, $r = |\mathbf{r}|$ is the magnitude of the radius vector, θ is the polar angle, and φ is the azimuthal angle in the spherical coordinate system (see the inset in Fig. 2). Indeed, the real spherical functions form a basis in space with scalar product given as integral of the solid angle

$$\langle Y_{p\ell m} | Y_{p'\ell'm'} \rangle = \int_{4\pi} Y_{p\ell m} Y_{p'\ell'm'} d\Omega = \delta_{p\ell m}^{p'\ell'm'}, \quad (6)$$

where $\delta_{p\ell m}^{p'\ell'm'}$ is a Kronecker delta, $\int_{4\pi} d\Omega \equiv \int_{\varphi=0}^{2\pi} \int_{\theta=0}^{\pi} \sin\theta d\theta d\varphi$. The multipole content of the mode (set of the nonzero $b_{p\ell m}$) can fully describe the mode properties, however, we leave the discussion of the multipole series' convergence and accuracy out of the scope of this paper saying that the precision is high enough for our purposes. We refer the reader to [76] where the numerical investigation of this problem is presented.

According to the Wigner theorem a specific eigenmode $p(\mathbf{r}, \omega)$ is transformed under particular irreducible representation of the resonator's symmetry group. Thus, in the expansion (5), only spherical functions which are transformed under this irreducible representation are presented. There cannot be any spherical functions transformed under different representation in the expansion. Accordingly, the problem of multipole expansion of eigenmodes of the resonator is reduced to determining from symmetry considerations under which irreducible representation a particular mode is transformed and finding a set of spherical harmonics $Y_{p\ell m}$, transformed through each other under the same one. To find such a set, the

(a)

D_{3h}	E	$2C_3(z)$	$3C_2'$	$\sigma_h(xy)$	$2S_3$	$3\sigma_v$
A'_1	+1	+1	+1	+1	+1	+1
A''_1	+1	+1	+1	-1	-1	-1
A'_2	+1	+1	-1	+1	+1	-1
A''_2	+1	+1	-1	-1	-1	+1
E'	+2	-1	0	+2	-1	0
E''	+2	-1	0	-2	+1	0

(b)

Mode examples	Irrep D_{3h}	Spherical Harmonics
	A'_1	Y_{e00} , Y_{e20} , Y_{e40} , $Y_{e(2l)(6m)}$, $Y_{e(2l-1)(6m-3)}$
	A''_1	Y_{o43} , Y_{o63} , Y_{o76} , $Y_{o(2l)(6m-3)}$, $Y_{o(2l-1)(6m)}$
	A'_2	Y_{o33} , Y_{o53} , Y_{o66} , $Y_{o(2l)(6m)}$, $Y_{o(2l-1)(6m-3)}$
	A''_2	Y_{e10} , Y_{e30} , Y_{e50} , $Y_{e(2l)(6m-3)}$, $Y_{e(2l-1)(6m)}$
	E'	Y_{o11} , Y_{e11} , Y_{o22} , $Y_{[e,o](2l)(6m-4)}$, $Y_{[e,o](2l)(6m-2)}$, $Y_{[e,o](2l-1)(6m-5)}$, $Y_{[e,o](2l-1)(6m-1)}$
	E''	Y_{o21} , Y_{e21} , Y_{o32} , $Y_{[e,o](2l)(6m-5)}$, $Y_{[e,o](2l)(6m-1)}$, $Y_{[e,o](2l-1)(6m-4)}$, $Y_{[e,o](2l-1)(6m-2)}$

FIG. 4. (a) Character table for symmetry group D_{3h} group. (b) Table of multipole composition of eigenmodes for a closed acoustic resonator of symmetry group D_{3h} : examples of modes transformed under particular irreducible representation (first column) and their multipolar content (third column).

projection operator on the irreducible representation is introduced \hat{P}_α [77,78]:

$$\hat{P}_\alpha = \frac{n_\alpha}{|G|} \sum_g \chi_\alpha^*(g) \hat{D}(g), \quad (7)$$

where $|G|$ is the order of the group, g is the group element, α is the number of irrep, n_α is the dimension of irrep, $\chi_\alpha^*(g)$ is the character of g , and $\hat{D}(g)$ is the transformation operator.

The operator \hat{P}_α projects arbitrary basis functions onto a linear combination of functions which are transformed under particular irreducible representation α [79]. Commonly, this procedure allows for the identification of the basis functions. However, for the case of the spherical functions set we can simply use the already obtained results and address the ready-made character tables [64,80]. With this, knowing that a particular eigenmode transforms under irrep α , one can immediately determine the multipole composition of this mode by simply finding the spherical functions, which are also transformed under the same irrep α . This set will determine the nonzero components in the expansion Eq. (5). For the resonators of D_{3h} symmetry, the multipolar content is shown in Fig. 4. The first column shows the results of numerical simulation obtained using an eigenmode solver in COMSOL MultiphysicsTM, where the color denotes the acoustical pressure at the surface of the resonator.

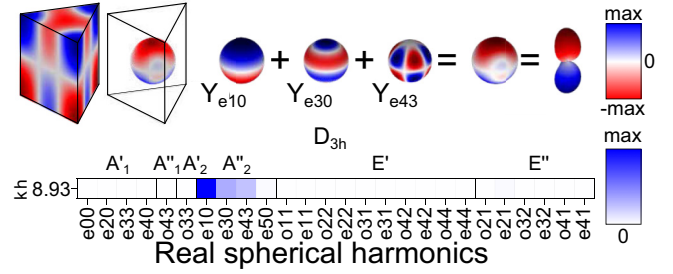


FIG. 5. Illustration of the analysis of the multipole composition of a particular eigenmode of a closed resonator. The integration of the pressure function of the eigenmode multiplied by the spherical function was performed over an auxiliary sphere inside the structure. The nonzero value of the integral (filled colored cells in the table) indicates that such a spherical function is included in the eigenmode expansion with a certain coefficient.

B. Numerical simulations

The group theory approach provides the nonzero multipole coefficients in the expansion Eq. (5). The quantitative analysis of these coefficients is usually carried out by direct multipole decomposition of the modes of open resonators [62]. Here, for the closed resonator under consideration, we are rather interested in testing the predicted nonzero multipole components based on the numerical simulations. For that, we numerically compute the pressure distributions of the eigenmode $p(\mathbf{r}, \omega)$ inside the resonator with the help of commercially available COMSOL MultiphysicsTM software. Then, the eigenmode function is multiplied by spherical harmonics $Y_{p\ell m}$ and integrated over a spherical surface embedded inside the resonator and with the center matching the resonator center of symmetry as shown in Fig. 5:

$$\begin{aligned} \langle p | Y_{p\ell m} \rangle &= \sum_{p', \ell', m'} b_{p' \ell' m'} \int_{4\pi} Y_{p' \ell' m'} Y_{p \ell m} d\Omega \\ &= \sum_{p', \ell', m'} c_{p' \ell' m'} \delta_{p \ell m}^{p' \ell' m'} = b_{p \ell m}. \end{aligned} \quad (8)$$

A nonzero result of the integration represents the fact that the spherical function is included to the eigenmode expansion (see Fig. 5 for a particular eigenmode of a prism resonator). The result will depend on the size of the sphere, however, we are interested in the zero values of the coefficients due to the symmetry restriction, which will stay zero for any sphere size.

Figure 6 summarizes the results of the symmetry analysis for different eigenmodes of D_{3h} group symmetry. It shows that for each eigenfrequency coefficients deviate from zero in one representation only. Moreover, there are degenerated modes in two-dimensional representations: two lines correspond to a single frequency and coefficients are in blocks or in a checker-board pattern. While finding the degenerate modes, the numerical solver often selects them in an arbitrary manner, however, by slightly violating the symmetry, we can force it to select a particular linear combination. The case of the checkerboard positioning corresponds to the case, where in each line every spherical function is either odd or even (Fig. 7), therefore one of the two degenerate modes is even when reflected in the $y = 0$ plane, and the second one is

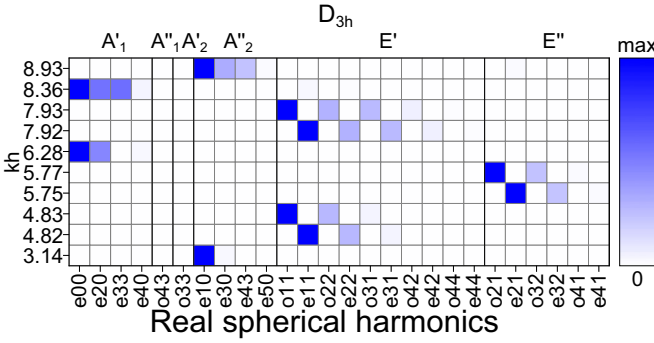


FIG. 6. A part of the infinite table of coefficients at spherical functions for the symmetry group D_{3h} . On the vertical axis, the product of the wave vector k of eigenmodes by the height h of the prism is given. The color saturation corresponds to the value of the coefficient $b_{p\ell m}$ in the expansion. The checkerboard arrangements correspond to degenerate modes transformed under two-dimensional representations of E' , E'' . The length of the horizontal base of the prism (object of symmetry group D_{3h}) is 44.68 mm and its height is 50 mm. However, geometrical properties are unimportant to this end.

odd. The checkerwise distribution can be achieved artificially by stretching the shape out along the x -axis. In this case the modes would not be truly degenerated due to the lower symmetry of the system, but their frequencies would be close enough.

C. Eigenmodes decomposition of closed resonators of different symmetry groups

As a next step, we performed the classification of resonators of other symmetry groups of D_{2h} , D_{3h} , D_{3d} , D_{4h} , D_{6h} , $D_{\infty h}$, C_{2v} , C_{3v} , C_{4v} , C_{6v} , $C_{\infty v}$ with customized geometrical parameters (see Appendix B). The tables for all symmetries are given in Appendix C in the form similar to Fig. 4.

D. Multipole content in the resonators of decreased symmetry

In this part, we would like to focus attention on an interesting behavior when lowering the symmetry of a resonator and correspondent multipoles' content evolution. In Fig. 8 the multipoles set of pyramid resonator (C_{4v} -group symmetry) is shown. Under particular transformation one can decrease its symmetry to C_{2v} , which is a subgroup of C_{4v} . When the symmetry is being lowered the number of irreducible representations is reduced: two one-dimensional represen-

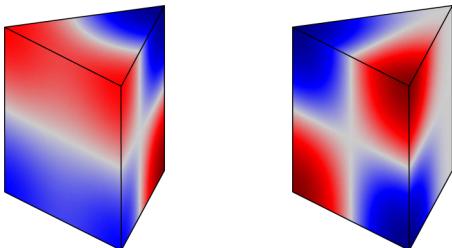


FIG. 7. Degenerated modes transformed under the irreducible representation E'' .

tations are merged, forming a different one-dimensional representation [23]. Moreover, degeneracies are canceled when the rotational symmetry around the z -axis is broken: two-dimensional representation turns to two one-dimensional, in other words two degenerated modes turn into two modes with different energies. In the following section, we will demonstrate the effect it has on the spectral features of acoustic wave scattering.

IV. ACOUSTIC WAVE SCATTERING

The scattering of an acoustic wave on the resonator with a particular set of eigenmodes results in the appearance of resonant features in the scattering spectrum. At this stage, the information on the particular multipole content of resonators can be extremely helpful to analyze and predict the spectral response of the resonant object.

In this section we used a particle with a particular set of qualities, such as size and material. As for the material, we implemented such set of density ($\rho = 1/\sqrt{6}$ kg/m³ for the particle and $\rho_0 = 1$ kg/m³ for the medium) and speed of sound ($c = 2$ m/s for the particle and $c_0 = 1$ m/s for the medium) that rendered an appearance of Mie resonances possible when the size of a particle is comparable with the wavelength. Thus, this set of qualities allowed us to call this particle a resonator.

On top of that, we used to regard the symmetry classification in closed resonator, however, it must be noted that in the scattering problem we will consider an open one. However, the symmetry of its eigenmodes will not change, therefore, the classification can still be applicable, aside from the fact that in this case modes will appear as quasinormal [81–84].

A. Multipoles expansion

We formulate the problem in the incident-scattered formalism, so the total fields are $(p_t, \mathbf{v}_t) = (p_{inc}, \mathbf{v}_{inc}) + (p_{sc}, \mathbf{v}_{sc})$. Radiation pressure of an incident plane acoustic wave, propagating along the z -axis is in the form of [11,16,17,75,85]

$$p_{inc} = p_0 e^{ikr \cos \theta} = \sum_{\ell=0}^{\infty} p_{\ell} j_{\ell}(kr) Y_{\ell 0}(\theta, \varphi), \quad (9)$$

where $p_{\ell} = p_0 i^{\ell} \sqrt{4\pi(2\ell+1)}$, p_0 is the incident wave amplitude, $j_{\ell}(kr)$ is the spherical Bessel function. By virtue of symmetry, there are solely spherical harmonics $m = 0$ presented in the expansion, however, for the scattered wave there might be all components in the expansion

$$p_{sc}(\mathbf{r}, \omega) = \sum_{p,\ell,m} a_{p\ell m}(\omega) h_{\ell}^{(1)}(kr) Y_{\ell m}(\theta, \varphi), \quad (10)$$

where $h_{\ell}^{(1)}$ is the spherical Hankel function of the first kind [86]. The scattering cross section can be expressed through the scattering coefficient as

$$\sigma_{sc} = \frac{1}{k^2} \sum_{p,\ell,m} |a_{p\ell m}(\omega)|^2 = \sum_{p,\ell,m} \sigma_{p\ell m}(\omega), \quad (11)$$

where $\sigma_{p\ell m}(\omega) = \frac{1}{k^2} |a_{p\ell m}(\omega)|^2$. The scattering cross section also can be obtained by direct integration of the scattered

Mode examples	a Irrep C_{4v}	Spherical Harmonics	Spherical Harmonics	b a Irrep C_{2v}	Mode examples
	A_1	Y_{e00} Y_{e10} Y_{e20} $Y_{e\ell(4m)}$	Y_{e00} Y_{e10} Y_{e20} $Y_{e\ell(2m)}$	A_1	
	A_2	Y_{o44} Y_{o54} Y_{o64} $Y_{o\ell(4m)}$	Y_{o22} Y_{o32} Y_{o42} $Y_{o\ell(2m)}$	A_2	
	B_1	Y_{e22} Y_{e32} Y_{e42} $Y_{e\ell(4m-2)}$	Y_{o11} Y_{o31} Y_{o43} $Y_{o\ell(2m-1)}$	B_1	
	B_2	Y_{o22} Y_{o32} Y_{o42} $Y_{o\ell(4m-2)}$	Y_{e11} Y_{e21} Y_{e31} $Y_{e\ell(2m-1)}$	B_2	
	E	Y_{e11} Y_{o11} Y_{e21} $Y_{[e,o]\ell(2m-1)}$			

FIG. 8. Two symmetry groups C_{4v} , C_{2v} , one of which is a subgroup of the other. Each irreducible representation corresponds to explicit examples of eigenmodes of the resonator transformed under given irreducible representation and expressed by a linear combination of spherical functions transformed under the same one. The blue arrows illustrate the reduction of the number of irreducible representations with decreasing symmetry and the red arrows show the cancellation of degeneracy with breaking the rotational symmetry around the z -axis by 90° . Geometry of studies closed resonators: $a = 50$ mm, $b = 20$ mm, overall height is 50 mm. For each resonator: density $\rho = 1190$ kg/m³, speed of sound $c = 2500$ m/c. However, geometrical properties are unimportant to this end.

wave energy flux over any surface surrounding the resonant object, for instance, a sphere of radius R ,

$$\sigma_{sc} = \frac{R^2}{I_0} \int_{4\pi} \frac{1}{2} \text{Re}(p_{sc}^* v_{sc,r}) d\Omega, \quad (12)$$

where I_0 is the incident wave intensity, v_r^s is the component of the local velocity of the scattered wave [87]. The answer does not depend on the integration sphere radius since the energy flux of the scatterer power $\frac{1}{2} \text{Re}(p_{sc}^* \mathbf{v}^s)|_{r=R} \propto 1/R^2$. The multipole expansion coefficients can be found by projecting the pressure of the scattered wave onto the corresponding spherical harmonic

$$\begin{aligned} (p_{sc}(\mathbf{r}, \omega) | Y_{\ell m}) &= \sum_{p', \ell', m'} a_{p' \ell' m'}(\omega) h_{\ell'}^{(1)}(kr) \int_{4\pi} Y_{p' \ell' m'} Y_{\ell m} d\Omega \\ &= \sum_{p', \ell', m'} a_{p' \ell' m'}(\omega) h_{\ell'}^{(1)}(kr) \delta_{p' \ell' m'}^{\ell m} \\ &= a_{\ell m}(\omega) h_{\ell}^{(1)}(kr). \end{aligned} \quad (13)$$

If the spherical function $Y_{\ell m}$ is included both in the incident wave expansion and in an eigenmode's expansion, then this eigenmode will be excited along with all others, which are transformed by the same irrep as $Y_{\ell m}$. Therefore, in the scattered wave the whole basis of spherical harmonics transformed under that irreducible representation is constituted. The incident plane wave propagating along the z -axis contains only spherical functions with $m = 0$ and, thus, it excites all modes which contain at least one spherical function with $m = 0$.

B. Acoustic scattering results

Let us now consider a particular case of wave scattering over an open acoustic resonator of C_{2v} and C_{4v} symmetry

groups. In accordance with the multipole analysis results mentioned earlier (Fig. 8), the incident wave excites only one irreducible representation, A_1 . However, irreducible representation A_1 for C_{2v} symmetry is a result of merging irreducible representations A_1 and B_1 of the C_{4v} symmetry group, therefore, irreducible representation A_1 for the C_{2v} symmetry group corresponds to $Y_{e\ell(2m)}$ spherical functions, while in the C_{4v} group there are only $Y_{e\ell(4m)}$ functions present. As a result, the multipole expansion of the wave scattered by the object with C_{2v} symmetry shows contributions of modes missing in the scattering on an object with C_{4v} symmetry (Fig. 9). The used parameters of the models and environment are presented in Appendix C.

C. Analogy to optics

Recently, the group symmetry analysis of eigenmodes and their multipolar content of the subwavelength optical resonator has been carried out in optics [62], where multipolar theory is a powerful tool for describing optical response of resonant nanostructures, predict, and design their optical properties [36,48,88,89]. The main difference between the optics and acoustics is that the electromagnetic fields are described by vector functions which adds a polarization degree of freedom. When considering the farfield multipolar

TABLE I. Relation between the multipole analysis in acoustics and optics.

Acoustics	Optics
Scalar spherical functions Y	Electric multipoles \mathbf{N}
—	Magnetic multipoles \mathbf{M}
	For a plane wave $k \parallel z$
Only $m = 0$	Only $m = 1$

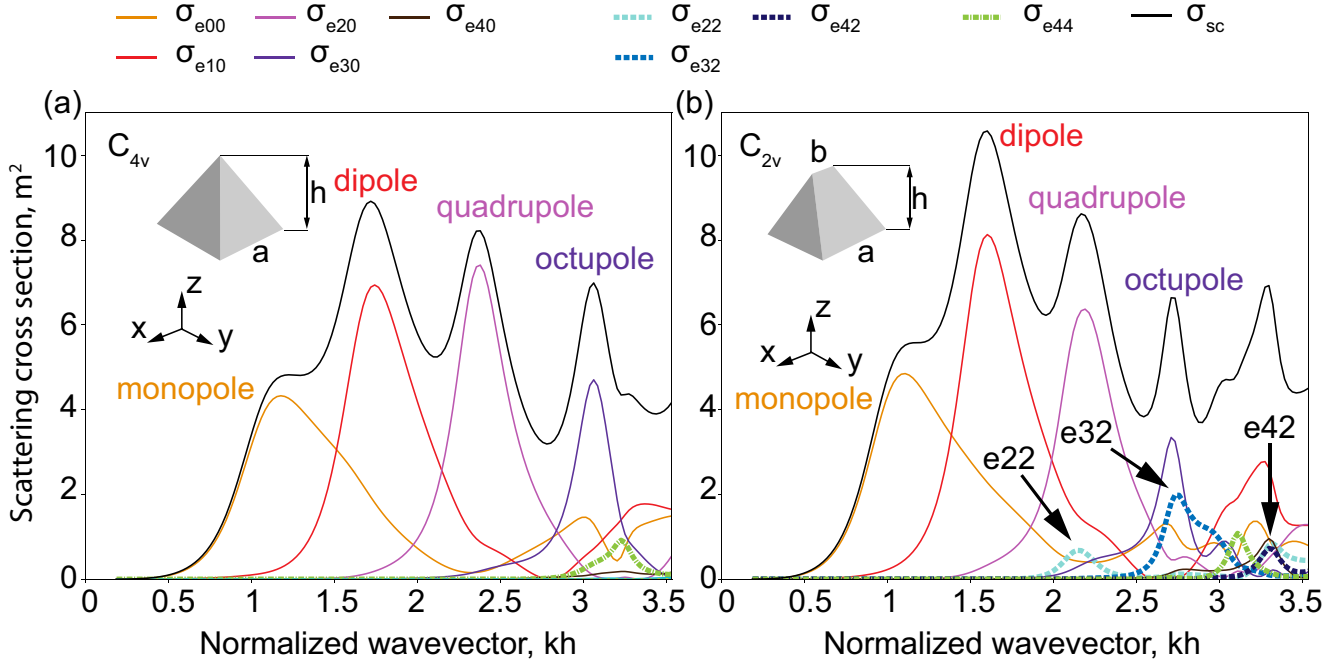


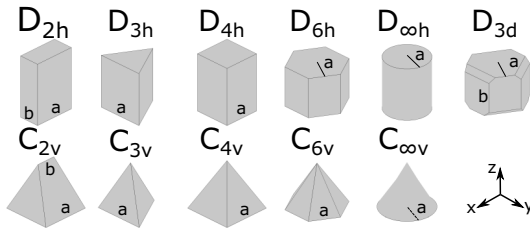
FIG. 9. Scattering cross-section expansion of two objects with (a) C_{4v} and (b) C_{2v} symmetries. Plane wave propagates along z -axis and therefore contains spherical harmonics with $m = 0$ only in its expansion. (b) The figure illustrates how a slight change of a symmetry alters the scattering spectrum multipolar content. Additional contributions of $Y_{\ell 2}$ are shown. Geometry parameters are $a = 1.5$ m, $b = 0.6$ m, overall height $h = 1.5$ m; parameters of the resonators: speed of sound $c = 2$ m/s, density $\rho = 1/\sqrt{6}$ kg/m³; parameters of the host medium: speed of sound $c_0 = 1$ m/s, density $\rho_0 = 1$ kg/m³.

content of the modes, one should consider two types of vector spherical harmonics — electric and magnetic ones. However, despite the complexity of electromagnetic modes, one can note that the content of the acoustic and optical modes is rather similar [62] as the electric multipoles behave almost exactly as the scalar spherical harmonics. The magnetic harmonics have opposite behavior under inversion and reflection, and can excite, for example, modes which transform under irreducible representations A_{2g} and A_{2u} in a cylinder, which is im-

possible in acoustics. Another important difference between acoustic and optical scattering is that the plane wave, incident along the z -axis, has only $m = 1$ due to the vector nature of the electromagnetic fields [90] and, thus, transforms under a different irreducible representation. Cylindrically symmetric optical fields with $m = 0$ can be achieved in vector beams. We summarize the correspondence between acoustics and optics in Table I.

V. CONCLUSION

Finally, in conclusion, we applied the machinery of group theory to classify and analyze the modes of subwavelength acoustic resonators in a way similar to nanophotonics. We considered the resonators eigenmodes of several symmetry groups (D_{2h} , D_{3h} , D_{3d} , D_{4h} , D_{6h} , $D_{\infty h}$, C_{2v} , C_{3v} , C_{4v} , C_{6v} , $C_{\infty v}$) and presented the classification tables of their eigenmodes and the multipolar content for each class. The



Parameter	D_{2h}	D_{3h}	D_{4h}	D_{6h}	$D_{\infty h}$	D_{3d}
h , mm	60	50	40	40	30	40
a , mm	40	44.68	25	25	12.5	25
b , mm	20					30
Parameter	C_{2v}	C_{3v}	C_{4v}	C_{6v}	$C_{\infty v}$	
h , mm	50	50	50	37.5	21.65	
a , mm	50	50	50	50	12.5	
b , mm	20					

FIG. 10. Geometry of studies closed resonators. h : overall height. For each resonator: density $\rho = 1190$ kg/m³, speed of sound $c = 2500$ m/c.

TABLE II. Parameters of the studied resonators and media in the Mie scattering problem.

Parameter	C_{4v}	C_{2v}	Host
h , m	1.5	1.5	
a , m	1.5	1.5	
b , m		0.6	
c , m/s	2	2	1
ρ , kg/m ³	$1/\sqrt{6}$	$1/\sqrt{6}$	1

Mode examples	Irrep D_{4h}	Spherical Harmonics	Mode examples	Irrep D_{2h}	Spherical Harmonics
	A_{1g}	Y_{e00} Y_{e20} Y_{e40} $Y_{e(2l)(4m)}$		A_g	Y_{e00} Y_{e20} Y_{e40} $Y_{e(2l)(2m)}$
	A_{2g}	Y_{o44} Y_{o64} $Y_{o(2l)(4m)}$		A_u	Y_{o32} Y_{o52} Y_{o54} $Y_{o(2l-1)(2m)}$
	A_{1u}	Y_{o54} Y_{o74} $Y_{o(2l-1)(4m)}$		B_{1g}	Y_{o22} Y_{o42} Y_{o44} $Y_{o(2l)(2m)}$
	A_{2u}	Y_{e10} Y_{e30} Y_{e50} $Y_{e(2l-1)(4m)}$		B_{2g}	Y_{e21} Y_{e41} Y_{e43} $Y_{e(2l)(2m-1)}$
	B_{1g}	Y_{e22} Y_{e42} Y_{e62} $Y_{e(2l)(4m-2)}$		B_{3g}	Y_{o21} Y_{o41} Y_{o43} $Y_{o(2l)(2m-1)}$
	B_{2g}	Y_{o22} Y_{o42} Y_{o62} $Y_{o(2l)(4m-2)}$		B_{1u}	Y_{e10} Y_{e30} Y_{e50} $Y_{e(2l-1)(2m)}$
	B_{1u}	Y_{o32} Y_{o52} Y_{o72} $Y_{o(2l-1)(4m-2)}$		B_{2u}	Y_{o11} Y_{o31} Y_{o33} $Y_{o(2l-1)(2m-1)}$
	B_{2u}	Y_{e32} Y_{e52} Y_{e72} $Y_{e(2l-1)(4m-2)}$		B_{3u}	Y_{e11} Y_{e31} Y_{e33} $Y_{e(2l-1)(2m-1)}$
	E_g	Y_{o21} Y_{e21} Y_{o41} $Y_{[e,o](2l)(2m-1)}$			
	E_u	Y_{o11} Y_{e11} Y_{o31} $Y_{[e,o](2l-1)(2m-1)}$			

Mode examples	Irrep D_{3d}	Spherical Harmonics	Mode examples	Irrep D_{3h}	Spherical Harmonics
	A_{1g}	Y_{e00} Y_{e20} Y_{e40} $Y_{e(2l)(6m)}$ $Y_{o(2l)(6m-3)}$		A'_1	Y_{e00} Y_{e20} Y_{e40} $Y_{e(2l)(6m)}$ $Y_{e(2l-1)(6m-3)}$
	A_{2g}	Y_{e43} Y_{e63} Y_{o66} $Y_{e(2l)(6m-3)}$ $Y_{o(2l)(6m)}$		A''_1	Y_{o43} Y_{o63} Y_{o76} $Y_{o(2l)(6m-3)}$ $Y_{o(2l-1)(6m)}$
	A_{1u}	Y_{e33} Y_{e53} Y_{o76} $Y_{e(2l-1)(6m-3)}$ $Y_{o(2l-1)(6m)}$		A'_2	Y_{o33} Y_{o53} Y_{o66} $Y_{o(2l)(6m)}$ $Y_{o(2l-1)(6m-3)}$
	A_{2u}	Y_{e10} Y_{e30} Y_{o73} $Y_{e(2l-1)(6m)}$ $Y_{o(2l-1)(6m-3)}$		A''_2	Y_{e10} Y_{e30} Y_{e50} $Y_{e(2l)(6m-3)}$ $Y_{e(2l-1)(6m)}$
	E_g	Y_{o21} Y_{e21} Y_{o22} $Y_{[e,o](2l)(3m-2)}$ $Y_{[e,o](2l)(3m-1)}$		E'	Y_{o11} Y_{e11} Y_{o22} $Y_{[e,o](2l)(6m-4)}$ $Y_{[e,o](2l)(6m-2)}$ $Y_{[e,o](2l-1)(6m-5)}$ $Y_{[e,o](2l-1)(6m-1)}$
	E_u	Y_{o11} Y_{e11} Y_{o31} $Y_{[e,o](2l-1)(3m-2)}$ $Y_{[e,o](2l-1)(3m-1)}$		E''	Y_{o21} Y_{e21} Y_{o32} $Y_{[e,o](2l)(6m-5)}$ $Y_{[e,o](2l)(6m-1)}$ $Y_{[e,o](2l-1)(6m-4)}$ $Y_{[e,o](2l-1)(6m-2)}$

FIG. 11. Tables of irreducible representations and examples of eigenmodes transformed under them and tables of characters of irreducible representations for symmetry groups D_{4h} , D_{2h} , D_{3d} , D_{3h} .

proposed multipole classification approach can be extended to any resonator shape and material. We connected the multipolar classification with the acoustic scattering problem since, by knowing only the multipolar structure of the incident wave and the symmetry group of the resonator, one can predict the exact multipolar composition of the scattered field. We studied in detail the lift of degeneracy in a

resonator of $C_{4v} \rightarrow C_{2v}$ symmetry and traced the evolution of the multipolar content as well as the reconfiguration the scattering spectrum. In particular, we showed that symmetry decreasing leads to expanding the range of multipoles in the scattered field. We believe that our result will find an application in rapidly developing acoustics of metamaterials and metaatoms.

Mode examples	Irrep $C_{\infty v}$	Spherical Harmonics	Mode examples	Irrep C_{6v}	Spherical Harmonics
	A_1	Y_{e00} Y_{e10} Y_{e20} $Y_{e\ell(0)}$		A_1	Y_{e00} Y_{e10} Y_{e20} $Y_{e\ell(6m)}$
	E_1	Y_{o11} Y_{e11} Y_{o21} $Y_{[e,o]\ell(1)}$		A_2	Y_{o66} $Y_{o\ell(6m)}$
	E_2	Y_{o22} Y_{e22} Y_{o32} $Y_{[e,o]\ell(2)}$		B_1	Y_{e33} Y_{e43} Y_{e53} $Y_{e\ell(6m-3)}$
	E_3	Y_{o33} Y_{e33} Y_{o43} $Y_{[e,o]\ell(3)}$		B_2	Y_{o33} Y_{o43} Y_{o53} $Y_{o\ell(6m-3)}$
	E_4	Y_{o44} Y_{e44} Y_{o54} $Y_{[e,o]\ell(4)}$		E_1	Y_{o11} Y_{e11} Y_{o21} $Y_{[e,o]\ell(6m-5)}$ $Y_{[e,o]\ell(6m-1)}$
...	...			E_2	Y_{o22} Y_{e22} Y_{o32} $Y_{[e,o]\ell(6m-4)}$ $Y_{[e,o]\ell(6m-2)}$

Mode examples	Irrep $D_{\infty h}$	Spherical Harmonics	Mode examples	Irrep D_{6h}	Spherical Harmonics
	A_{1u}	Y_{e10} Y_{e30} Y_{e50} $Y_{e(2\ell-1)(0)}$		A_{1g}	Y_{e00} Y_{e20} Y_{e40} $Y_{e(2\ell)(6m)}$
	A_{1g}	Y_{e00} Y_{e20} Y_{e40} $Y_{e(2\ell)(0)}$		A_{2g}	Y_{o66} $Y_{o(2\ell)(6m)}$
	E_{1u}	Y_{o11} Y_{e11} Y_{o31} $Y_{[e,o](2\ell-1)(1)}$		A_{1u}	Y_{o76} $Y_{o(2\ell-1)(6m)}$
	E_{2u}	Y_{o32} Y_{e32} Y_{o52} $Y_{[e,o](2\ell-1)(2)}$		A_{2u}	Y_{e10} Y_{e30} Y_{e50} $Y_{e(2\ell-1)(6m)}$
	E_{3u}	Y_{o33} Y_{e33} Y_{o53} $Y_{[e,o](2\ell-1)(3)}$		B_{1g}	Y_{o43} Y_{o63} $Y_{o(2\ell)(6m-3)}$
	E_{1g}	Y_{o21} Y_{e21} Y_{o41} $Y_{[e,o](2\ell)(1)}$		B_{2g}	Y_{e43} Y_{e63} $Y_{e(2\ell)(6m-3)}$
	E_{2g}	Y_{o22} Y_{e22} Y_{o42} $Y_{[e,o](2\ell)(2)}$		B_{1u}	Y_{e33} Y_{e53} $Y_{e(2\ell-1)(6m-3)}$
	E_{3g}	Y_{o43} Y_{e43} Y_{o63} $Y_{[e,o](2\ell)(3)}$		B_{2u}	Y_{o33} Y_{o53} $Y_{o(2\ell-1)(6m-3)}$
...	...			E_{1g}	Y_{o21} Y_{e21} Y_{o41} $Y_{[e,o](2\ell)(6m-5)}$ $Y_{[e,o](2\ell)(6m-1)}$
				E_{2g}	Y_{o22} Y_{e22} Y_{o42} $Y_{[e,o](2\ell)(6m-4)}$ $Y_{[e,o](2\ell)(6m-2)}$
				E_{1u}	Y_{o11} Y_{e11} Y_{o31} $Y_{[e,o](2\ell-1)(6m-5)}$ $Y_{[e,o](2\ell-1)(6m-1)}$
				E_{2u}	Y_{o32} Y_{e32} Y_{o52} $Y_{[e,o](2\ell-1)(6m-4)}$ $Y_{[e,o](2\ell-1)(6m-2)}$

FIG. 12. Tables of irreducible representations and examples of eigenmodes transformed under them, and tables of characters of irreducible representations for symmetry groups $C_{\infty v}$, C_{6v} , $D_{\infty h}$, D_{6h} .

ACKNOWLEDGMENTS

The authors would like to thank Yuri Kivshar for the fruitful discussions. The symmetry analysis was supported by the Russian Science Foundation (Project No. 22-42-04420), while the numerical simulations were supported by the Russian Science Foundation (Project No. 20-72-10141). K.F. and M.P. acknowledge support from the Foundation for the Advancement of Theoretical Physics and Mathematics ‘‘BASIS’’ (Russia). This research was supported by Priority 2030 Federal Academic Leadership Program.

APPENDIX A: ACOUSTICS MASTER EQUATIONS FOR THE MEDIA WITH COORDINATE-DEPENDENT PARAMETERS

Fundamental equations for the linear monochromatic acoustics are [70–72,91]

$$\begin{cases} i\omega\rho\mathbf{v} = \nabla p & \text{linearized Navier-Stokes equation,} \\ i\omega\beta p = \nabla \cdot \mathbf{v} & \text{equation of continuity,} \\ p = c^2\rho & \text{equation of state.} \end{cases} \quad (\text{A1})$$

Once there is a medium with coordinate-dependent mass density $\rho = \rho(\mathbf{r})$ and compressibility $\beta = \beta(\mathbf{r})$ the single master equation for the pressure field without external sources is going to be [[92], Sec. 2.1],[[91], Sec. 8.1]

$$\nabla^2 p + \frac{\omega^2}{c^2(\mathbf{r})} p = \frac{\nabla\rho}{\rho} \cdot \nabla p, \quad (\text{A2})$$

here $c = 1/\sqrt{\beta\rho}$ is the speed of sound.

APPENDIX B: COMSOL MULTIPHYSICS™ MODEL

We used EIGENVALUE SOLVER to observe the electromagnetic fields of closed resonators. We established a spherical domain inside the resonator (Fig. 5) to estimate the $b_{\rho\ell m}$ coefficient in the multipole expansion (8). We integrate pressure and spherical harmonics (6) over the surface of the sphere

$$b_{\rho\ell m} = \int_{4\pi} p(\mathbf{r}) Y_{\rho\ell m} d\Omega. \quad (\text{B1})$$

We used a built-in complex form of spherical harmonics to get a real solution (2).

For the open resonator we used the FREQUENCY DOMAIN SOLVER. The model geometry is a sphere with a perfect matched layer (PML) domain and resonator at the center. To get $a_{\rho\ell m}(\omega)$ (13) we integrated the scalar product of far-field scattering pressure p^s and spherical harmonics over a concentric parametric surface with a radius R outside of the resonator, but inside the PML sphere as follows:

$$a_{\rho\ell m}(\omega) = \frac{1}{h_\ell^{(1)}(kR)} \int_{4\pi} p_{sc}(\mathbf{r}, \omega) Y_{\rho\ell m} d\Omega. \quad (\text{B2})$$

We also note that in Eq. (B2) one should use $h_\ell^{(2)}$ in COMSOL MULTIPHYSICS™ instead of $h_\ell^{(1)}$. This comes from the fact the outgoing wave should have the asymptotics as e^{-ikr} once the $e^{+i\omega t}$ convention is used, which is the case for the COMSOL

Mode examples	Irrep C_{2v}	Spherical Harmonics
	A_1	Y_{e00} , Y_{e10} , Y_{e20} , $Y_{e\ell(2m)}$
	A_2	Y_{o22} , Y_{o32} , Y_{o42} , $Y_{o\ell(2m)}$
	B_1	Y_{o11} , Y_{o31} , Y_{o43} , $Y_{o\ell(2m-1)}$
	B_2	Y_{e11} , Y_{e21} , Y_{e31} , $Y_{e\ell(2m-1)}$

Mode examples	Irrep C_{3v}	Spherical Harmonics
	A_1	Y_{e00} , Y_{e10} , Y_{e20} , $Y_{e\ell(3m)}$
	A_2	Y_{o33} , Y_{o43} , Y_{o53} , $Y_{o\ell(3m)}$
	E	Y_{e11} , Y_{o11} , Y_{e21} , $Y_{e\ell(3m-2)}$, $Y_{e\ell(3m-1)}$

Mode examples	Irrep C_{4v}	Spherical Harmonics
	A_1	Y_{e00} , Y_{e10} , Y_{e20} , $Y_{e\ell(4m)}$
	A_2	Y_{o44} , Y_{o54} , Y_{o64} , $Y_{o\ell(4m)}$
	B_1	Y_{e22} , Y_{e32} , Y_{e42} , $Y_{e\ell(4m-2)}$
	B_2	Y_{o22} , Y_{o32} , Y_{o42} , $Y_{o\ell(4m-2)}$
	E	Y_{e11} , Y_{o11} , Y_{e21} , $Y_{e\ell(2m-1)}$

FIG. 13. Tables of irreducible representations and examples of eigenmodes transformed under them and tables of characters of irreducible representations for symmetry groups C_{2v} , C_{3v} , C_{4v} .

MULTIPHYSICS™. The sum of the squared absolute values of the coefficients equals σ_{sc} (11).

We used the same concentric parametric surfaces to get σ_{sc} by Eq. (12). The following expression was used as an integrand in COMSOL MULTIPHYSICS™ model (built-in acoustics interfaces notation)

$$0.5*\text{realdot}(\text{acpr.p}_s, (-(d(\text{acpr.p}_s, x))*x) + (-(d(\text{acpr.p}_s, y))*y) + (-(d(\text{acpr.p}_s, z))*z))/(\text{acpr.rho}_c*\text{acpr.iomega}))$$

APPENDIX C: MODELS AND GEOMETRY OF STUDIED CLOSED RESONATORS

In this section, we provide the parameters of the resonators we study, which are given in Fig. 10. For all these shapes we provide the multipolar decomposition.

In Table II, we present the parameters of the studied resonators, which we discuss in scattering problem.

APPENDIX D: EIGENMODES' MULTIPOLE DECOMPOSITION RESULTS

In this section, we provide the multipolar classification of resonators' modes. In Fig. 11 the symmetry groups of the resonators are D_{4h} , D_{2h} , D_{3d} , and D_{3h} . In Fig. 12 – $C_{\infty v}$, C_{6v} , $D_{\infty h}$, and D_{6h} . In Fig. 13 – C_{2v} , C_{3v} , and C_{4v} .

-
- [1] G. Ma and P. Sheng, *Sci. Adv.* **2**, e1501595 (2016).
- [2] J. Guo, X. Zhang, Y. Fang, and R. Fattah, *J. Appl. Phys.* **124**, 104902 (2018).
- [3] A. Melnikov, Y. K. Chiang, L. Quan, S. Oberst, A. Alù, S. Marburg, and D. Powell, *Nat. Commun.* **10**, 3148 (2019).
- [4] S. A. Cummer, J. Christensen, and A. Alù, *Nat. Rev. Mater.* **1**, 16001 (2016).
- [5] C. Liu, J. Shi, W. Zhao, X. Zhou, C. Ma, R. Peng, M. Wang, Z. H. Hang, X. Liu, J. Christensen, N. X. Fang, and Y. Lai, *Phys. Rev. Lett.* **127**, 084301 (2021).
- [6] A. Melnikov, M. Maeder, N. Friedrich, Y. Pozhanka, A. Wollmann, M. Scheffler, S. Oberst, D. Powell, and S. Marburg, *J. Acoust. Soc. Am.* **147**, 1491 (2020).
- [7] M. Krasikova, Y. Baloshin, A. Slobozhanyuk, A. Melnikov, D. Powell, M. Petrov, and A. Bogdanov, *AIP Conf. Proc.* **2300**, 020069 (2020).
- [8] T. Brunet, A. Merlin, B. Mascaro, K. Zimny, J. Leng, O. Poncelet, C. Aristégui, and O. Mondain-Monval, *Nat. Mater.* **14**, 384 (2015).
- [9] T. Yamamoto, *J. Appl. Phys.* **123**, 215110 (2018).
- [10] N. Dostart, Y. Liu, and M. A. Popović, *Sci. Rep.* **7**, 17509 (2017).
- [11] I. D. Toftul, K. Y. Bliokh, M. I. Petrov, and F. Nori, *Phys. Rev. Lett.* **123**, 183901 (2019).
- [12] X. Ni, M. Li, M. Weiner, A. Alù, and A. B. Khanikaev, *Nat. Commun.* **11**, 2108 (2020).
- [13] X. Ni, M. Weiner, A. Alù, and A. B. Khanikaev, *Nat. Mater.* **18**, 113 (2019).
- [14] A. S. Pilipchuk, A. A. Pilipchuk, and A. F. Sadreev, *Phys. Scr.* **95**, 085002 (2020).
- [15] D. N. Maksimov, A. F. Sadreev, A. A. Lyapina, and A. S. Pilipchuk, *Wave Motion* **56**, 52 (2015).
- [16] B. Slovick and S. Krishnamurthy, *Appl. Phys. Lett.* **113**, 223106 (2018).
- [17] V. C. Anderson, *J. Acoust. Soc. Am.* **22**, 426 (1950).
- [18] A. Clebsch, *De Gruyter* **1863**, 195 (1863).
- [19] L. Lorenz, *Eur. Phys. J. H* **44**, 77 (2019).
- [20] G. Mie, *Ann. Phys. (Leipzig)* **330**, 377 (1908).
- [21] L. Landau and E. Lifshitz, *Quantum Mechanics: Non-Relativistic Theory*, Course of Theoretical Physics (Elsevier Science, Amsterdam, 1981).
- [22] E. L. Ivchenko and G. Pikus, in *Crystal Symmetry*, Springer Series in Solid-State Sciences, edited by E. L. Ivchenko and G. Pikus (Springer, New York, 1995), pp. 9–38.
- [23] M. S. Dresselhaus, G. Dresselhaus, and A. Jorio, *Group Theory. Application to the Physics of Condensed Matter* (Springer, New York, 2008).
- [24] G. F. Koster, *Properties of the Thirty-Two Point Groups*, Vol. 24 (MIT Press, Cambridge, MA, 1963).
- [25] S. Hayami, M. Yatsushiro, Y. Yanagi, and H. Kusunose, *Phys. Rev. B* **98**, 165110 (2018).
- [26] Z. Zhang, Z.-M. Yu, G.-B. Liu, and Y. Yao, [arXiv:2201.11350](https://arxiv.org/abs/2201.11350).
- [27] J. Mei, Y. Wu, C. T. Chan, and Z.-Q. Zhang, *Phys. Rev. B* **86**, 035141 (2012).
- [28] N. Laforge, R. Wiltshaw, R. V. Craster, V. Laude, J. A. Iglesias Martínez, G. Dupont, S. Guenneau, M. Kadic, and M. P. Makwana, *Phys. Rev. Appl.* **15**, 054056 (2021).
- [29] A. Cammarata, *RSC Adv.* **9**, 37491 (2019).
- [30] S. Reich, N. S. Mueller, and M. Bubula, *ACS Photonics* **7**, 1537 (2020).
- [31] K. Frizyuk, *J. Opt. Soc. Am. B* **36**, F32 (2019).
- [32] K. Frizyuk, I. Volkovskaya, D. Smirnova, A. Poddubny, and M. Petrov, *Phys. Rev. B* **99**, 075425 (2019).
- [33] T. Cao, M. Wu, and S. G. Louie, *Phys. Rev. Lett.* **120**, 087402 (2018).
- [34] A. C. Overvig, S. C. Malek, M. J. Carter, S. Shrestha, and N. Yu, *Phys. Rev. B* **102**, 035434 (2020).
- [35] R. Yang, S. Yue, Y. Quan, and B. Liao, *Phys. Rev. B* **103**, 184302 (2021).
- [36] D. Smirnova and Y. S. Kivshar, *Optica* **3**, 1241 (2016).
- [37] Y. Kivshar and A. Miroshnichenko, *Opt. Photonics News* **28**, 24 (2017).
- [38] S. Kruk and Y. Kivshar, *ACS Photonics* **4**, 2638 (2017).
- [39] S. D. Krasikov, M. A. Odit, D. A. Dobrykh, I. M. Yusupov, A. A. Mikhailovskaya, D. T. Shakirova, A. A. Shcherbakov, A. P. Slobozhanyuk, P. Ginzburg, D. S. Filonov, and A. A. Bogdanov, *Phys. Rev. Appl.* **15**, 024052 (2021).
- [40] J. J. Faran, Jr., *J. Acoust. Soc. Am.* **23**, 405 (1951).
- [41] H. Esfahlani, Y. Mazor, and A. Alù, *Phys. Rev. B* **103**, 054306 (2021).
- [42] D. A. Kovacevich and B.-I. Popa, *Phys. Rev. B* **104**, 134304 (2021).
- [43] C. F. Sieck, A. Alù, and M. R. Haberman, *Phys. Rev. B* **96**, 104303 (2017).
- [44] D. Torrent and J. Sánchez-Dehesa, *Phys. Rev. B* **79**, 174104 (2009).
- [45] J.-P. Sessarego, J. Sageloli, R. Guillermin, and H. Überall, *J. Acoust. Soc. Am.* **104**, 2836 (1998).
- [46] J. S. Bolton and T. A. Beauvilain, *J. Acoust. Soc. Am.* **91**, 2349 (1992).
- [47] L. Meng, F. Cai, F. Li, W. Zhou, L. Niu, and H. Zheng, *J. Phys. D* **52**, 273001 (2019).
- [48] T. Liu, R. Xu, P. Yu, Z. Wang, and J. Takahara, *Nanophotonics* **9**, 1115 (2020).

- [49] Y. Cheng, C. Zhou, B. G. Yuan, D. J. Wu, Q. Wei, and X. J. Liu, *Nat. Mater.* **14**, 1013 (2015).
- [50] X. Zhu, B. Liang, W. Kan, Y. Peng, and J. Cheng, *Phys. Rev. Appl.* **5**, 054015 (2016).
- [51] I. Toftul, K. Bliokh, and M. Petrov, *AIP Conf. Proc.* **2300**, 020127 (2020).
- [52] E. B. Lima and G. T. Silva, *J. Acoust. Soc. Am.* **150**, 376 (2021).
- [53] K. Rehfeld, *Materials and Corrosion* **29**, 79 (1978).
- [54] L. Wei and F. J. Rodríguez-Fortuño, *New J. Phys.* **22**, 083016 (2020).
- [55] G. Lu, E. Ding, Y. Wang, X. Peng, J. Cui, X. Liu, and X. Liu, *Appl. Phys. Lett.* **110**, 123507 (2017).
- [56] Z. Gong and M. Baudoin, *J. Acoust. Soc. Am.* **149**, 3469 (2021).
- [57] A. Santillán and S. I. Bozhevolnyi, *Phys. Rev. B* **84**, 064304 (2011).
- [58] D. Saparov, B. Xiong, Y. Ren, and Q. Niu, *Phys. Rev. B* **105**, 064303 (2022).
- [59] Z. Wang, D. Liu, H. T. Teo, Q. Wang, H. Xue, and B. Zhang, *Phys. Rev. B* **105**, L060101 (2022).
- [60] S. J. Ippolito, A. Trinchi, D. A. Powell, and W. Wlodarski, in *Solid State Gas Sensing* (Springer, Boston, 2008), pp. 1–44.
- [61] K. Ohtaka and Y. Tanabe, *J. Phys. Soc. Jpn.* **65**, 2670 (1996).
- [62] S. Gladyshev, K. Frizyuk, and A. Bogdanov, *Phys. Rev. B* **102**, 075103 (2020).
- [63] Z. Xiong, Q. Yang, W. Chen, Z. Wang, J. Xu, W. Liu, and Y. Chen, *Opt. Express* **28**, 3073 (2020).
- [64] A. Gelessus, W. Thiel, and W. Weber, *J. Chem. Educ.* **72**, 505 (1995).
- [65] W. Hergert and R. M. Geilhufe, Spherical harmonics, in *Group Theory in Solid State Physics and Photonics* (John Wiley & Sons, New York, 2018), pp. 331–336.
- [66] Character table for point group $D_{\infty h}$ (Online accessed 21 April 2022), <http://symmetry.jacobs-university.de/cgi-bin/group.cgi?group=1001&option=4>.
- [67] W. Fulton and J. Harris, *Representation Theory* (Springer-Verlag, New York, 2004).
- [68] D. A. Varshalovich, A. N. Moskalev, and V. K. Khersonsky, *Quantum Theory of Angular Momentum: Irreducible Tensors, Spherical Harmonics, Vector Coupling Coefficients, 3nj Symbols* (World Scientific, Singapore, 1988).
- [69] A. Piróth and J. Sólyom, *Fundamentals of the Physics of Solids* (Springer, Berlin, 2007).
- [70] L. D. Landau and E. M. Lifshitz, *Fluid Mechanics: Landau and Lifshitz: Course of Theoretical Physics, Volume 6* (Elsevier, Amsterdam, 2013).
- [71] H. Bruus, *Lab Chip* **11**, 3742 (2011).
- [72] H. Bruus, *Lab Chip* **12**, 20 (2012).
- [73] A. A. Bogdanov, K. L. Koshelev, P. V. Kapitanova, M. V. Rybin, S. A. Gladyshev, Z. F. Sadrieva, K. B. Samusev, Y. S. Kivshar, and M. F. Limonov, *Adv. Photonics* **1**, 016001 (2019).
- [74] M. B. Doost, W. Langbein, and E. A. Muljarov, *Phys. Rev. A* **90**, 013834 (2014).
- [75] E. G. Williams, *Fourier Acoustics: Sound Radiation and Nearfield Acoustical Holography* (Academic, New York, 1999).
- [76] B. Auguié, W. R. C. Somerville, S. Roache, and E. C. L. Ru, *J. Opt.* **18**, 075007 (2016).
- [77] X. Zheng, N. Verellen, D. Vercruyse, V. Volskiy, P. Van Dorpe, G. A. E. Vandenbosch, and V. Moshchalkov, *IEEE Trans. Antennas Propag.* **63**, 1589 (2015).
- [78] R. S. Knox and A. Gold, *Symmetry in the Solid State* (W.A. Benjamin, New York, 1964).
- [79] P. J. Olver, *Classical Invariant Theory* (Cambridge University Press, Cambridge, England, 1999).
- [80] G. Katzer, Character tables for point groups C_n , C_{nv} , C_{nh} , D_n , D_{nh} , D_{nd} , S_{2n} etc. (Online accessed 21 April 2022), http://www.gernot-katzers-spice-pages.com/character_tables/index.html.
- [81] J. Kergomard, V. Debut, and D. Matignon, *J. Acoust. Soc. Am.* **119**, 1356 (2006).
- [82] V. Cardoso, J. P. S. Lemos, and S. Yoshida, *Phys. Rev. D* **70**, 124032 (2004).
- [83] P. Lalanne, W. Yan, K. Vynck, C. Sauvan, and J.-P. Hugonin, *Laser Photonics Rev.* **12**, 1700113 (2018).
- [84] E. S. C. Ching, P. T. Leung, A. Maassen van den Brink, W. M. Suen, S. S. Tong, and K. Young, *Rev. Mod. Phys.* **70**, 1545 (1998).
- [85] P. Martin, *Wave Motion* **86**, 63 (2019).
- [86] Z. Gong, P. L. Marston, and W. Li, *Phys. Rev. E* **99**, 063004 (2019).
- [87] Z. Gong, W. Li, Y. Chai, Y. Zhao, and F. G. Mitri, *Ocean Eng.* **129**, 507 (2017).
- [88] R. Raab and O. De Lange, *Multipole Theory in Electromagnetism: Classical, Quantum and Symmetry Aspects, with Applications* (Oxford Science Publications, Oxford, 2005), p. 248.
- [89] Z. Sadrieva, K. Frizyuk, M. Petrov, Y. Kivshar, and A. Bogdanov, *Phys. Rev. B* **100**, 115303 (2019).
- [90] C. F. Bohren and D. R. Huffman, *Absorption and Scattering of Light by Small Particles* (John Wiley & Sons, New York, 1998).
- [91] D. Colton and R. Kress, *Inverse Acoustic and Electromagnetic Scattering Theory* (Springer, New York, 2013).
- [92] A. A. Gorunov and A. V. Saskovets, *Inverse Scattering Problems in Acoustics (in Russian)* (Moscow State University, Moscow, 1989).